Magnetic Resonance in Antiferromagnetic $FeCl_2 \cdot 4H_2O$†

D. D. THORNTON*‡
Syracuse University, Syracuse, New York 13210
(Received 17 November 1969)

The electronic magnetic resonance spectrum of single crystals of $FeCl_2 \cdot 4H_2O$ has been studied in the microwave region from 9 to 76 GHz at temperatures between 0.38 and 4.2 K. Two distinct types of resonance characteristic of the antiferromagnetic state were observed, each of which is associated with a pair of highly anisotropic g tensors ($g_1 \simeq 0$) with principal axes $\pm 30°$ from the b axis in the a'-b plane. One of these resonance pairs is easily distinguishable from the other, since its integrated resonance intensity is some three orders of magnitude larger. It is an unusual antiferromagnetic resonance in that the frequency-field relation is temperature-independent, whereas the resonance intensity is strongly temperature-dependent. The intensity is greatest at the lowest temperatures and decreases rapidly as the Néel temperature is approached, with a small remanent signal observable even above T_N. The zero-field resonance was observed at 72.5 GHz. No spin-flop resonance was observed. The weak-intensity resonances, which we denote as Ising spin resonances because of the very large g anisotropy, are similar in some respects to the spin-cluster resonances observed in $CoCl_2 \cdot 2H_2O$ and $FeCl_2$, but are characterized by a strong local antiferromagnetic interaction rather than the dominant ferromagnetic interaction of those other materials. Resonances corresponding to many of the possible local spin configurations were measured, and the temperature dependence of the resonance intensities was determined. In addition, resonances associated with a small concentration of Mn impurities were observed.

I. INTRODUCTION

THE elementary excitations of an ordered magnetic system are commonly described as quantized spin waves, i.e., magnons in which a single spin reversal is shared by the entire spin system. In a perfectly isotropic Heisenberg system the magnon excitation spectrum extends continuously to zero energy. The presence of anisotropy introduces into this spectrum an energy gap whose magnitude is largely dependent upon the degree of anisotropy. In contrast, the excitations in an Ising system are single spin reversals which are localized to a single site. Thus, only the exchange and Zeeman interactions determine the magnitude of the excitation. In the following these excitations will be referred to as Ising excitations and the associated resonances as Ising spin resonance (ISR). One might expect that in a system with a crystalline-field anisotropy which was large compared with the exchange and Zeeman interactions, it might be possible to observe Ising excitations as well as spin waves. A third form of excitation which may occur in an ordered magnetic system are the localized magnon modes associated with magnetic impurities.

Some form of each of these modes of excitation has been observed in various antiferromagnetic compounds. Antiferromagnetic resonance (AFMR) is just the excitation of the uniform precession mode ($k=0$ magnons), and has been observed in the majority of low-T_N antiferromagnets. ISR is much less common and only recently has been observed in $CoCl_2 \cdot 2H_2O$ [1,2] and $FeCl_2$.[3] Impurity resonance has also been observed in these materials.[3,4]

This paper presents the results of a microwave resonance study of $FeCl_2 \cdot 4H_2O$ in which all three types of resonance have been observed.[5] The observed behavior of the AFMR is considerably different from that generally encountered in the hydrated transition-metal halides with regard to the temperature and magnetic field dependences. It appears that the usual molecular-field approach fails to provide an adequate explanation of these resonances. The ISR also takes a different form from that observed in $CoCl_2 \cdot 2H_2O$ and $FeCl_2$. In those salts the magnetic structure involves ferromagnetic chains or sheets in an antiferromagnetic array; the resonances thus correspond to ferromagnetic clusters flipping in the exchange field of their neighbors as well as the applied field. The magnetic structure of $FeCl_2 \cdot 4H_2O$ consists of antiferromagnetic chains in an antiferromagnetic array, so that no clustering effect is observed. There are, however, a variety of exchange environments in which a spin may flip, resulting in a number of zero-field splittings for these resonances.

A number of earlier studies of the magnetic properties of ferrous-chloride tetrahydrate have also revealed interesting and unusual magnetic behavior at low temperatures. These experiments include specific-heat and magnetic susceptibility determinations, proton NMR

† Work supported in part by National Science Foundation.
* NASA Traineeship 1964–1967; Xerox Fellow 1967–1968.
‡ Presently NRC-NBS Postdoctoral Fellow at National Bureau of Standards, Washington, D. C. 20234.

[1] M. Date and M. Motokawa, Phys. Rev. Letters **16**, 111 (1966); M. Date and M. Motokawa, J. Phys. Soc. Japan **24**, 41 (1968).
[2] J. B. Torrance, Jr., and M. Tinkham, J. Appl. Phys. **39**, 822 (1968).
[3] M. Date and M. Motokawa, J. Appl. Phys. **39**, 820 (1968).
[4] M. Motokawa and M. Date, J. Phys. Soc. Japan **23**, 1216 (1967).
[5] D. D. Thornton and A. Honig, Bull. Am. Phys. Soc. **13**, 688 (1968).

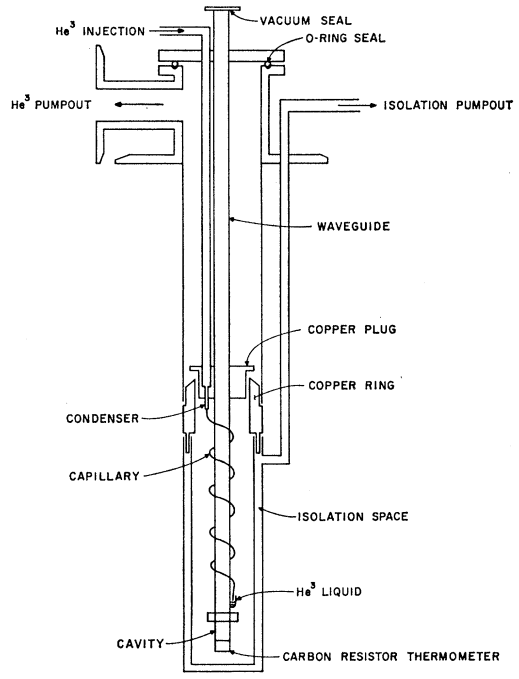

FIG. 1. Schematic of He^3 cryostat. Access to refrigerator and sample involves only one room-temperature O-ring seal.

measurements, as well as adiabatic magnetization and Mössbauer-effect studies.[6–12] It will be useful to summarize briefly the known magnetic properties of this material.

Above 20 K the magnetic susceptibility follows a Curie-Weiss law with $\theta=2$ K and an isotropic g factor of 2.19. The single-crystal susceptibility is highly anisotropic in the liquid-helium region and exhibits features characteristic of antiferromagnetism: The parallel (b axis) susceptibility has a broad maximum at about 1.5 K, while the perpendicular (c axis) susceptibility is nearly constant from about 1.5 to 0.3 K. However, the parallel susceptibility extrapolates to a small but finite value at 0 K and is greater than the perpendicular susceptibility above 0.7 K.[8] The specific heat has been measured between 1.15 and 20 K,[6] and more recently down to 0.4 K.[7] A sharp λ anomaly at 1.097 K indicates the onset of long-range order at this temperature. At higher temperatures, there is a well-defined Schottky anomaly which has a broad maximum at about 3.0 K. The height of the Schottky hump indicates that there are two low-lying states well separated from three higher levels. The susceptibility results have been used to obtain a model of the Fe^{2+} ground state, which is consistent with the specific-heat data. In addition, the susceptibility results form the basis of a model of the antiferromagnetic ground state of $FeCl_2 \cdot 4H_2O$.[13]

The proton NMR has been observed from 4.2 to 0.37 K.[9] Above 1.1 K the spectrum is characteristic of the paramagnetic state, while below 0.7 K the proton lines are split by local fields into 16 components whose behavior indicates the presence of four magnetic sublattices ordered antiferromagnetically. These results are consistent with the model constructed by Uryû.[13] Between 0.7 and 1.1 K, the resonance lines are not observed at all. However, the Mössbauer studies show that there are no further phase changes below 1.1 K. Also, the Mössbauer experiments indicate the sublattice magnetization reaches near saturation quite rapidly, changing by only about 4% below 0.9 K.[11,12] Recent adiabatic magnetization experiments indicate that there may be a spin-flop transition below about 0.76 K in applied fields of about 5.5 kOe.[10]

The results to be reported here provide some additional information regarding the magnetic structure and interactions of this system. In addition, they contain implications regarding the general applicability of present theories of the elementary excitations of antiferromagnetically ordered systems.

II. EXPERIMENTAL

Most of the experiments to be described here were performed between 0.38 and 4.2 K at frequencies from 16.5 to 75 GHz in a He^3 microwave cryostat. Additional experiments limited to temperatures above 0.95 K were carried out between 9 and 12 GHz. The He^3 cryostat is shown schematically in Fig. 1. The body of the cryostat consists of the He^3 pumping tube, the lower portion of which includes a vacuum jacket for thermal isolation between the low-temperature region and the 1 K bath. The K-band waveguide, He^3 condenser, and evaporator form a unit easily removed from the body of the cryostat. Thus, access to both the refrigerator and the sample involves only one room-temperature seal. Thermal contact between the pumped He^4 bath and the He^3 condenser was maintained by a copper foil pressed between the condenser plug and the condenser ring, both made of copper.

The sample was mounted in the microwave cavity at the bottom of the waveguide, where it was cooled by the gas evolving from the pumped pool of liquid He^3. This method of thermal contact necessitated the use of very low microwave power levels in order to assure that the sample was in thermal equilibrium with both the He^3 bath and the carbon-resistance thermometer. The

[6] S. A. Friedberg, A. F. Cohen, and J. H. Schelleng, J. Phys. Soc. Japan **17**, 515 (1962).
[7] C. A. Raquet and S. A. Friedberg, Bull. Am. Phys. Soc. **12**, 339 (1967).
[8] J. T. Schriempf and S. A. Friedberg, Phys. Rev. **136**, A518 (1964).
[9] R. D. Spence, R. Au, and P. A. Van Dalen, Physica **30**, 1612 (1964).
[10] J. N. McElearney, H. Forstat, and P. T. Bailey, Phys. Rev. **181**, 887 (1969).
[11] C. E. Johnson and M. S. Ridout, J. Appl. Phys. **38**, 1272 (1967).
[12] K. Ono, M. Shinohara, A. Ito, T. Fujita, and A. Ishigaki, J. Appl. Phys. **39**, 1126 (1968).
[13] N. Uryû, Phys. Rev. **136**, A527 (1964).

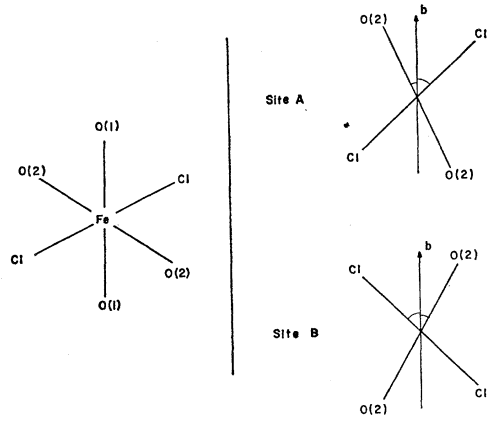

FIG. 2. Arrangement of a molecular group is shown on the left. The 0(1)-0(1) axis is perpendicular to the plane containing the O(2) and Cl ions. On the right is shown the relative configurations of the A and B groups projected on the a'-b plane. Distances are given in Angstroms.

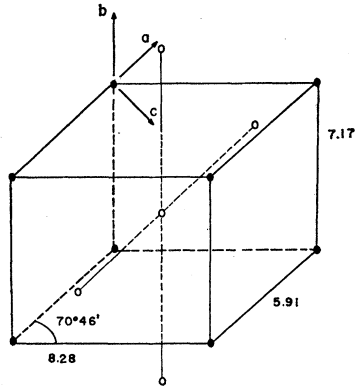

FIG. 3. Body-centered unit cell with the second nearest neighbors of the center ion also shown.

temperature dependence of the ISR intensity was very pronounced, and so provided a sensitive measure of the effects of microwave heating.

The low-intensity Ising spin and impurity resonances were detected with the usual field modulation and lock-in detection schemes. However, the large dispersion which accompanied the high-intensity AFMR detuned the cavity considerably, even with the smallest samples. Consequently, it was necessary to use the techniques discussed by Abkowitz and Honig[14] to measure the resonant field and to obtain the line shapes.

Samples were single crystals of $FeCl_2 \cdot 4H_2O$ grown from aqueous solution. There were three different methods of preparation which resulted in three different levels of sample purity. Those grown from solution prepared from commercial Reagent Grade chemical were found to have a relative concentration of 0.15% manganese impurity. A subsequent batch of samples was intentionally doped to about 0.46% Mn, while a third batch was grown from a solution prepared from 99.999% pure iron. When the samples were removed from solution, they were washed and sealed in pressure sensitive Teflon tape to prevent decomposition. When not in use the samples were stored at dry-ice temperatures. The crystals were oriented using the natural growth habit as a guide. This method was checked by examining the crystals under a polarization microscope. The over-all uncertainty in orientation was about $\pm 10°$, although it was possible to position the b-c plane with an uncertainty of less than $\pm 5°$ as this is a natural growth plane of the crystal.

III. CRYSTALLOGRAPHY

The crystal structure of $FeCl_2 \cdot 4H_2O$ is monoclinic with a space group $P2_1/c$ ($a=5.91$ Å, $b=7.17$ Å, $c=8.44$ Å, and $\beta=112°10'$).[15] There are two distinct $FeCl_2 \cdot 4H_2O$ molecular groups per unit cell with each Fe^{2+} ion coordinated by the four H_2O groups and the two Cl^- ions in a distorted octahedron. The arrangement of one of the groups is shown in Fig. 2; the other is related to the one shown by a mirror reflection in the b-c plane of the crystal. The point-group symmetry at the Fe sites is also monoclinic with the principal monoclinic axis (0(1)-0(1)) very nearly parallel to the c axis of the crystal. Labeling one of the inequivalent sublattices A and the other B, it is necessary to define two coordinate systems. The 0(1)-0(1) axis is chosen as a common y^A, y^B axis, the local spin axes of the respective sublattices are defined as z^A and z^B, while the x^A and x^B axes are then chosen to assure right-handed orthogonal coordinate systems. The macroscopic coordinate system is completely defined in terms of the crystallographic data. The monoclinic b axis is taken as the Z coordinate, while the c and a' axes form the Y and X coordinates, respectively. Note that this system does not coincide exactly with the principal macroscopic axes of the susceptibility tensor in that the c and a' axes make an angle of 5° with the principal axes determined by Schriempf and Friedberg.[8] Figure 3 shows the body-centered unit cell with the second nearest neighbors of the center ion included. If the ion in the center is a B ion, then it has four A nearest neighbors at 5.54 Å and four A third nearest neighbors at 6.84 Å; in addition, there are two B second nearest neighbors at 5.91 Å along the a axis.

IV. THEORY

A. Ground State of Ferrous Ion

The electronic configuration of the ferrous ion consists of six ($3d$) electrons around an argon core. The orbital degeneracy of the ^5D ground term is completely lifted by the low point-group symmetry potential of the distorted coordination octahedra. The spin-orbit

[14] M. Abkowitz and A. Honig, Phys. Rev. **136**, A1003 (1964).

[15] B. R. Penfold and J. A. Grigor, Acta Cryst. **12**, 850 (1959).

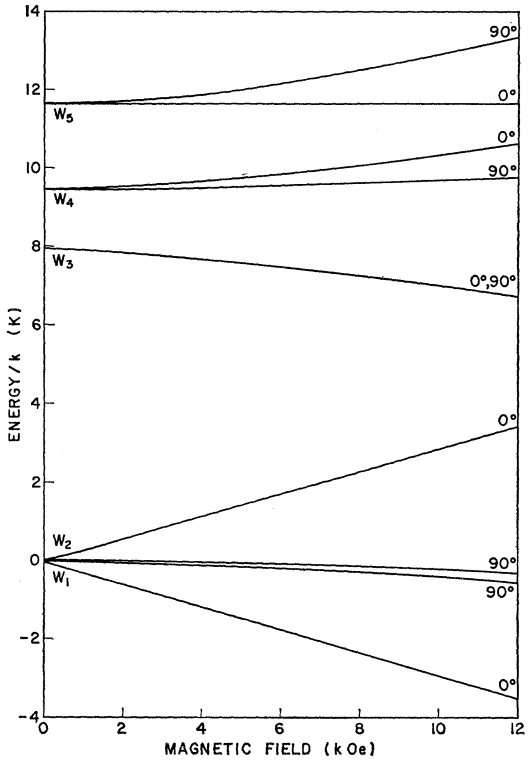

FIG. 4. Magnetic field dependence of the energy levels of the Fe^{2+} ion in a rhombic crystalline field. The solution labeled 0° is for a field applied along the $z(z^{A,B})$ axis and 90° is for a field applied along the $x(x^{A,B})$ axis.

coupling then removes the fivefold spin degeneracy of the orbital ground state as well as admixing small amounts of the excited orbital states. Since the spin-orbit coupling is much smaller than the crystal-field splitting of the orbital states (100 cm^{-1}/1000 cm^{-1}), the ground spin quintuplet may be described by a spin Hamiltonian formalism.

Tinkham has discussed the problem of the Fe^{2+} ion in an octahedral environment with a small rhombic distortion.[16] In the analysis of the susceptibility data for $FeCl_2 \cdot 4H_2O$, Schriempf and Friedberg use the Hamiltonian proposed by Tinkham:

$$\mathcal{H}=D[S_z^2-\tfrac{1}{3}S(S+1)]+E(S_x^2-S_y^2) +\mu_B \sum_i^{x,y,z} g_i H_i S_i. \quad (1)$$

The crystal-field parameters appearing in the spin Hamiltonian depend upon the choice of coordinate system, but in terms of the microscopic system defined in Sec. III, Schriempf and Friedberg obtain

$$\begin{aligned} D&=-2.895k, & g_x&=2.20, \\ E&=-0.255k, & g_y&=2.21, \\ & & g_z&=2.16, \end{aligned} \quad (2)$$

[16] M. Tinkham, Proc. Roy. Soc. (London) **A236**, 535 (1956).

where k is the Boltzmann constant. In the absence of an external field, the spin Hamiltonian may be readily diagonalized to give the following eigenvalues and eigenvectors:

$$\begin{aligned} &W_1=-2D[1-(1+\eta^2)^{1/2}], \\ &\phi_1=(1/\sqrt{2})\cos\alpha\,(|2\rangle+|-2\rangle)+\sin\alpha\,|0\rangle, \\ &W_2=0, \\ &\phi_2=(1/\sqrt{2})(|2\rangle-|-2\rangle), \\ &W_3=-3D+3E, \\ &\phi_3=(1/\sqrt{2})(|1\rangle+|-1\rangle), \\ &W_4=-3D-3E, \\ &\phi_4=(1/\sqrt{2})(|1\rangle-|-1\rangle), \\ &W_5=-2D[1+(1+\eta^2)^{1/2}], \\ &\phi_5=(1/\sqrt{2})\sin\alpha\,(|2\rangle+|-2\rangle)+\cos\alpha\,|0\rangle, \end{aligned} \quad (3)$$

where

$$\tan\alpha=[1+(1+\eta^2)^{1/2}]^{-1}, \quad \eta=\sqrt{3}(E/D).$$

The problem is somewhat more involved in the presence of an applied field. It is possible to obtain a "complete" solution numerically with the aid of a computer, and the results of such a calculation are shown in Fig. 4. With the choice of parameters (2), $\phi_{1,2}$ form a low-lying doublet which is widely separated from the three higher levels as shown in the figure. Owing to the large separation from the higher spin levels, this low doublet may itself be treated in an effective spin approximation for ordinary magnetic fields. The Hamiltonian in the pseudospin, $S'=\frac{1}{2}$, is

$$\mathcal{H}'=g_{\parallel}\mu_B S_z' H_z+\Delta S_x', \quad (4)$$

where

$$\Delta\equiv W_2-W_1\approx\eta^2 D \quad \text{and} \quad g_{\parallel}=4g_z(1-\tfrac{1}{8}\eta^2).$$

Such a spin is clearly a very close approximation to an Ising spin, since $g_\perp=0$.

B. AFMR

At this point it is possible to proceed in two, quite disparate directions: (a) the molecular-field approach in which the normal modes of the sublattice magnetization vectors are expressed in terms of the various effective fields; (b) the Ising model, suggested by the Hamiltonian (4), in which the excitations would correspond to the transitions of a spin in all of the possible configurations with its neighbors. In this subsection we investigate the first of these methods, reserving the latter for Sec. IV C.

An aggregation of spins coupled together by an exchange interaction possesses collective modes of excitation known as spin waves. In the presence of some form of anisotropy, the lowest-energy mode, the uniform precession, occurs at a finite energy determined largely by the magnitude of the anisotropy. There have been a number of theoretical studies aimed at obtaining the

spin-wave, or magnon, frequencies in terms of the microscopic parameters such as the exchange constants and the anisotropy constants. Most of these studies invoke some form of molecular-field theory to make the connection between the microscopic and macroscopic problems.

In a simple two-sublattice uniaxial antiferromagnet with crystalline-field anisotropy, the frequency of the uniform precession is given by the expression

$$h\nu = g\mu_B(H_A^2 + 2H_E H_A)^{1/2}. \quad (5)$$

H_A and H_E are the "effective" fields usually expressed in terms of the molecular-field constants K and A:

$$H_A = \frac{K}{M} = \frac{2K}{Ng\mu_B\langle S\rangle}, \quad H_E = AM = \tfrac{1}{2}Ng\mu_B A\langle S\rangle, \quad (6)$$

where $\langle S\rangle$ is the thermal average of the spin expectation value. The molecular-field constants are then the parameters which must be expressed in terms of the microscopic constants. Such expressions have been derived[17,18] for this simple case:

$$K = \tfrac{1}{2}NDS(S-\tfrac{1}{2}), \quad A = 2zJ/N(g\mu_B)^2, \quad (7)$$

where z is the number of nearest neighbors and μ_B is the Bohr magneton. In principle, J and D may be determined independently, or J may be determined independently and D is then determined by the AFMR experiment.

A second approach ignores the microscopic problem completely, but gains generality in so doing. This is the phenomenological approach of Kanamori and Tachiki[19] in which the AFMR frequency is related directly to other experimentally determined quantities

$$h\nu = g\mu_B(2K/\chi_\perp)^{1/2}. \quad (8)$$

These results are only directly applicable to a uniaxial two-sublattice antiferromagnet. Although $FeCl_2 \cdot 4H_2O$ has a four-sublattice structure, two independent two-sublattice systems would result if the first- and third-neighbor interactions were negligible.

The molecular-field approach is a well-defined method and has been reasonably successful in explaining AFMR experiments in the past. The Uryû model of the $FeCl_2 \cdot 4H_2O$ ground state provides an excellent starting point for the application of this method. Unfortunately, the field-dependent problem is quite involved and requires a numerical solution. A preliminary calculation along these lines has been performed with the aid of a computer and the results plotted in Fig. 5. The values of the various parameters appearing in the calculation were those used by Uryû.

[17] J. Kanamori and H. Minatono, J. Phys. Soc. Japan **17**, 1759 (1962).
[18] T. Nagamiya, K. Yosida, and R. Kubo, Advan. Phys. **4**, 2 (1955).
[19] J. Kanamori and M. Tachiki, J. Phys. Soc. Japan **17**, 1384 (1962).

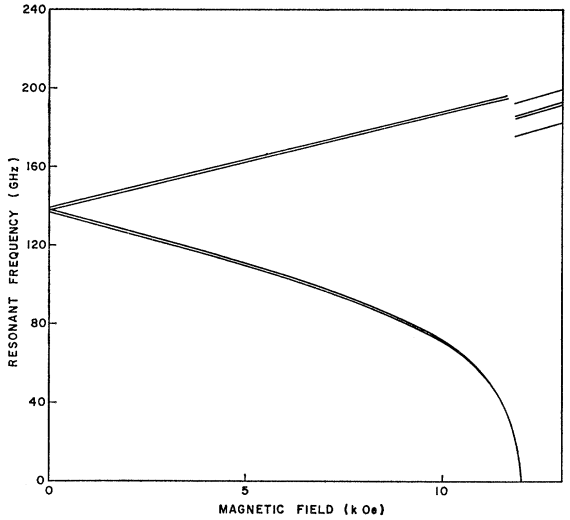

FIG. 5. Normal modes for the four-sublattice model calculated using a semiclassical molecular-field approach. The field is parallel to the b axis.

In the presence of sufficiently high applied magnetic fields, the antiferromagnetic state is no longer stable and the magnetic system will undergo a transition into a new state of lower free energy. If the exchange energy is larger than the anisotropy energy and the latter is not too large, the system can undergo a "spin-flop" transition in which the difference vector ($\mathbf{\Delta} \equiv \mathbf{S}_1 - \mathbf{S}_2$) of the sublattice spins "flops" from a direction parallel to the applied field to a direction perpendicular to the field. The condition for spin flop is determined by the difference in the magnetic free energy of the normal and flopped states. When this difference exceeds the anisotropy energy, spin flop will occur; thus, the critical field H_c is determined by

$$\tfrac{1}{2}\chi_\perp H_c^2 - \tfrac{1}{2}\chi_{11}H_c^2 = M_0 H_A = K \quad (9)$$

or

$$H_c = [2K/(\chi_\perp - \chi_{11})]^{1/2}.$$

It should be pointed out that $\chi_\perp$ is meant to be the susceptibility perpendicular to the difference vector $\mathbf{\Delta}$. Thus, the derivation of (9) implies that the exchange energy is much greater than the anisotropy energy. If the crystalline-field anisotropy is comparable to the exchange energy, it will affect the magnitude of $\chi_\perp$ and $\chi_\perp$ should be referred to the crystal axis. Then, $\chi_\perp$ is no longer appropriate to use in calculating the induced moment in the spin-flop phase.

C. ISR

A completely different picture is obtained by assuming that, as suggested by (4), the individual spins may be approximated by Ising spins. Since there are no transverse interactions in an Ising system the usual collective spin-wave excitations do not appear. Instead, the excitations correspond to individual spin reversals. The types of excitation that could occur in a linear

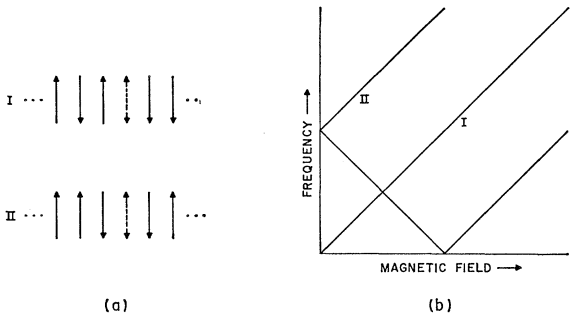

FIG. 6. (a) Possible spin configurations in which a spin may flip in a linear antiferromagnetic chain. (b) Frequency-field diagram for situation (a).

chain of antiferromagnetically coupled Ising spins are shown in Fig. 6 with the corresponding frequency-field diagram. A more complicated system with more possible configurations will have a correspondingly greater number of resonance branches and zero-field splittings. If up to third nearest-neighbor exchange interactions are significant in the $FeCl_2 \cdot 4H_2O$ system, there are 35 possible resonance branches with 17 corresponding zero-field splittings, ignoring the small splitting of the doublet itself. The resonance branches may be represented by taking all possible combinations in the following expression:

$$\delta_1 = 2S^2 \begin{Bmatrix} 0 & 0 & 0 \\ 2J_1 & +2J_3 & +2J_2 \\ 4J_1 & 4J_3 & \end{Bmatrix} \pm g\mu_B SH, \qquad (10)$$

where the values of g and S are those appropriate to the effective spin.

The Ising model is primarily a statistical model and may be used to calculate the expected temperature dependence of the intensity of the ISR. The absorption intensity of the resonances of this type of system should be proportional to the magnetization, and thus should have the same temperature dependence. Although the linear antiferromagnetic Ising chain is not a particularly good approximation to the system under consideration, it possesses the singular virtue that its magnetization

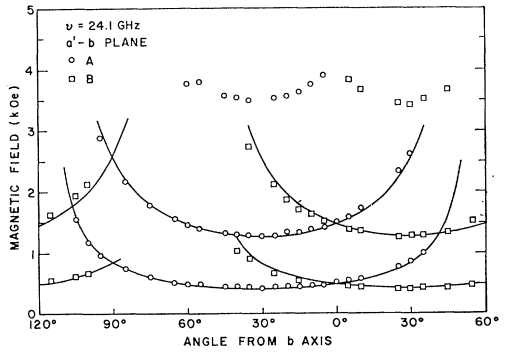

FIG. 7. Angular dependence of the ISR in the a'-b plane. The solid curves are for vanishing g_1.

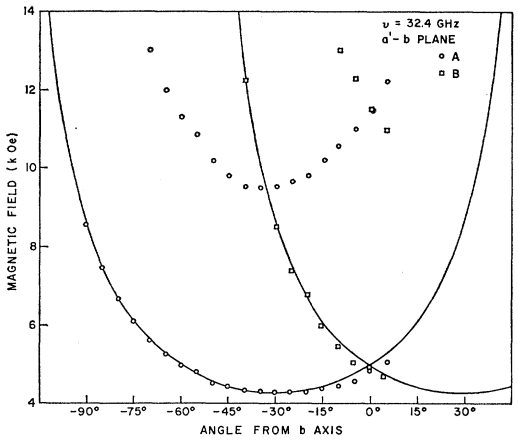

FIG. 8. Angular dependence of the two AFMR in the a'-b plane. Solid curves are for vanishing g_1.

may simply be calculated in closed form. The resultant expression is

$$M = \tfrac{1}{2} N g \mu_B \frac{\sinh(g\mu_B H/kT)}{[\sinh^2(g\mu_B H/kT) + \exp(4J/kT)]^{1/2}}. \qquad (11)$$

It is unlikely that (11) would give the actual dependence of the magnetization in the three-dimensional system, particularly near the transition. However, the exponential decrease at low temperatures seems to be a characteristic feature which might be observed.

The Ising model, with its complete lack of transverse coupling, is a very special system in that a spin reversal is localized to a single lattice site. The presence of even a small amount of transverse coupling tends to spread a spin reversal over the spin system as a whole. It would appear, therefore, that even in systems closely approximating Ising systems an appropriate description would have to be based ultimately upon a spin-wave approach. A step in this direction has been taken by Torrance and Tinkham[20] in discussing the multiple magnon excitations, or "cluster" resonances observed in $CoCl_2 \cdot 2H_2O$. As yet, however, there has been no attempt to extend this approach to systems in which the dominant interactions were antiferromagnetic.

V. RESULTS

The microwave absorption spectrum of single crystals of $FeCl_2 \cdot 4H_2O$ has been investigated from 8 to 76 GHz in applied magnetic fields up to 13 kOe. and over the temperature range from 0.38 to 4.2 K. Three distinct types of resonance were observed: impurity resonance, ISR, and AFMR. The impurity resonance was not studied in the same detail as the others. For both ISR and AFMR the frequency-field relation was determined as well as the temperature and orientational dependences.

[20] J. B. Torrance, Jr., and M. Tinkham, Phys. Rev. **187**, 587 (1969).

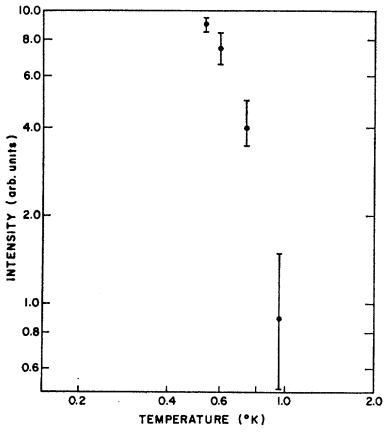

FIG. 9. Intensity of the Mn impurity resonance as a function of temperature.

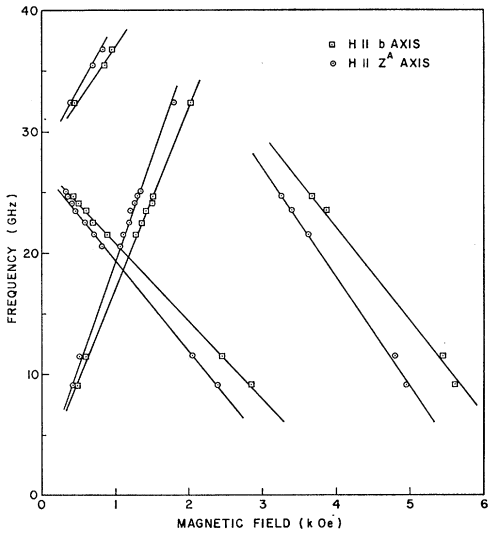

FIG. 10. Frequency dependence of the ISR of the A system plotted for applied field parallel to z^A and to the b axis. $T \simeq 0.6$°K.

The angular dependence of the ISR and the AFMR are shown in Figs. 7 and 8. The solid curves have been calculated using two independent g tensors, each possessing only one nonzero component. The principal axis of each tensor was taken to be in the a'-b plane and to make an angle of 30° with the b axis. Thus, these resonances exhibit the orientation dependence expected of the Fe^{2+} ion. Experiments in other orientations indicate that the a'-b plane is a symmetry plane.

A. Impurity Resonance

The impurity resonances were first observed at K band in the original samples grown from Reagent Grade chemical. In these samples the intensity was quite low and the lines could be observed only at the lowest temperatures. At 24 GHz there were four nearly equally spaced lines with the lowest of these occurring at zero field. The splitting of about 110 Oe and the apparent g factor were roughly isotropic in the a'-b plane. Spectroscopic analysis indicated the presence of manganese impurity with a relative concentration of 0.15%. In samples doped with a relative concentration of 0.46% Mn, these resonance lines displayed a threefold increase in relative single strength. In samples prepared from 99.999% pure iron, these lines were not observed. The signals from the doped samples were intense enough to permit observation of the temperature dependence. The resonance condition was independent of temperature, but the signal strength varied rapidly with temperature as shown in Fig. 9. The linewidth was about 50 Oe. It is interesting that these impurity lines were observed only in the antiferromagnetic region.

B. ISR

These were the weak Fe^{2+} resonance lines. Although they were somewhat stronger than the Mn lines, the optimum signal to noise was about 20/1. A comparison of the maximum intensity at 24 GHz with a calibrated sample of diphenylpicrylhydrazyl (DPPH) indicated that only about 10^{-3} to 10^{-4} of the Fe^{2+} spins were involved.

Four principal resonance branches were observed for each of the two inequivalent systems A and B. Several weaker "satellites" appeared within a few hundred Oe of each main line, but the very low intensity prevented any meaningful assignment of these lines. The frequency-field data for the ISR corresponding to the A system are plotted in Fig. 10 for a magnetic field applied along the z^A axis as well as for one applied along the b axis. The resonance condition was not observed to change with temperature. Both the zero-field splitting and the g factor were different for each branch. The observed values are listed in Table I. Each branch also had a different linewidth, which in all cases was between 30 and 100 Oe for H_0 parallel to z^i and increased with the angle between H_0 and z.

Although the other properties of the ISR were largely temperature-independent, the signal intensity exhibited a characteristic strong dependence upon the temperature. As shown in Fig. 11, the intensity was a maximum at 0.65 K and fell off rapidly as the temperature was either raised or lowered. Here, as with the impurity resonances, the resonance lines were observed only in the ordered region.

TABLE I. Values of g and the zero-field splitting for the observed branches of the Ising spin resonance shown in Fig. 10.

Branch	g	Zero-field splitting (GHz)
I	12.3	2
II	5.4	27
III	7.8	29.3
IV	6.5	53.5

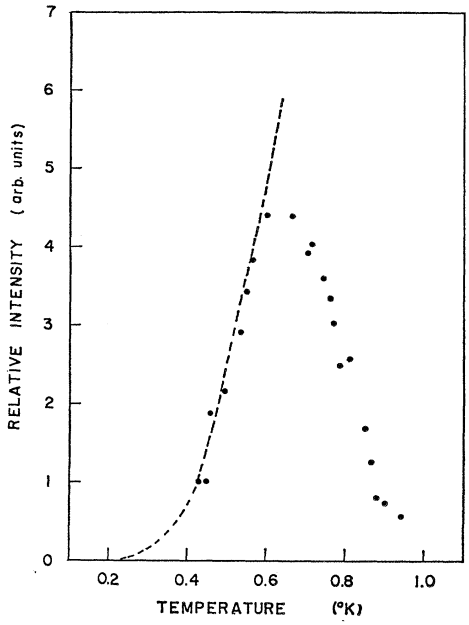

FIG. 11. Variation of ISR intensity with temperature. Dotted curve shows the temperature dependence of the net magnetization of an antiferromagnetic Ising chain with $J/k=1.3$ K.

C. AFMR

These were the strong Fe^{2+} resonance lines. Nearly 1000 times more intense than the ISR, these resonances visually detuned the cavity absorption and required an entirely different mode of detection. They have been observed over the frequency range from 9 to 75 GHz and at temperatures from 0.4 to 1.5 K. There are two resonance branches for each of the inequivalent magnetic sites as shown in Fig. 8. Although the resonance condition of these lines appears to be independent of temperature, the intensities have a pronounced temperature dependence with each branch exhibiting a characteristic behavior. Above T_N the low-field resonance is a residual bump on a general low-field absorption as shown in Fig. 12. The general absorption decreases slowly below T_N, but the resonance line itself does not increase significantly until the temperature is less than 0.7 K. The high-field line, however, is more intense than the low-field line above T_N, but it increases in a more gradual manner as the temperature is lowered. At low temperatures the low-field linewidth is about 200 Oe, while the high-field linewidth is nearly 500 Oe; in both cases the applied field is parallel to the z axis. The temperature dependence of the absorption intensities is shown in Fig. 13.

VI. DISCUSSION

Both the ISR and AFMR exhibit the large anisotropy and large g values expected of the Fe^{2+} ion. In other respects, notably the absorption intensity, these resonances were dramatically different, even though

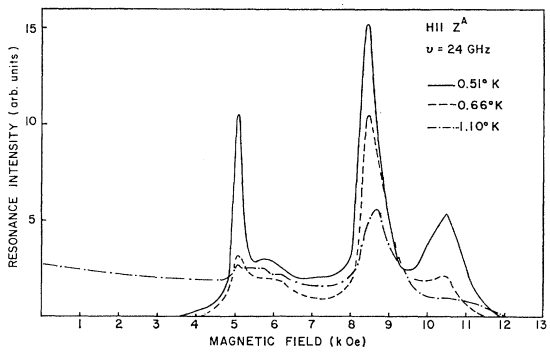

FIG. 12. Absorption intensity of the AFMR versus applied field for various temperatures.

both are associated with the antiferromagnetic state. These large differences suggest that the two phenomena might be more simply treated as distinct rather than unified. This suggestion is reinforced by the lack of a theory broad enough to describe the type of system encountered here. Consequently, the results will be discussed in terms of the two disparate models described in Sec. IV following a brief discussion of the impurity resonances.

A. Impurity Resonances

The impurity resonances observed in samples grown from commercially obtained reagent is attributed to residual manganese. A spectroscopic study has revealed that manganese is the only significant metallic impurity in these crystals, appearing in a relative concentration of about 0.15%. This conclusion is consistent with the threefold increase in intensity of these lines relative to the Fe^{2+} lines in a sample doped to 0.46% Mn, as well as their absence from samples prepared from pure iron.

The Mn^{2+} ion is in a ${}^6S_{5/2}$ ground state so that the g factor is expected to be isotropic and approximately 2.0, as was observed. In addition Mn^{55} has a nuclear spin of $\frac{5}{2}$. It is possible to observe either a fine structure of five nearly equally spaced lines[21] or a hyperfine structure of six equally spaced lines, or both, depending upon the relative magnitudes of the crystal field and hfs interactions. In this instance it is difficult to tell conclusively which structure is being observed. The difficulty arises because the frequency at which the impurity resonances were observed was approximately equal to the zero-field splitting caused by the Mn-Fe exchange. Thus, the resonance pattern was "folded" at zero field, with the result that only four lines were observed. However, at resonance positions where two lines overlapped, the observed lines ought to have twice the intensity of a normal line. Since this was observed for two of the lines of the pattern suggesting a total of six lines, it appears that hyperfine interaction is the cause of the splitting.

[21] W. Low, *Paramagnetic Resonance in Solids* (Academic Press Inc., New York, 1960), pp. 113–121.

B. Ferrous Ion

The description of the ground state of the Fe^{2+} ion in $FeCl_2 \cdot 4H_2O$ which was developed from the susceptibility and specific-heat data indicates that below 3 K nearly all of the ions would be in the ground doublet represented by (4). The g tensor of this manifold has a single nonvanishing component, $g_{II}=4g_z(1-\frac{1}{8}\eta^2)$. The inequivalent A and B ions have different principal spin axes and corresponding g tensors, differing only by a reflection through the b-c plane. The resonance results show that the local spin axes lie in the a'-b plane at an angle of $\pm 30°$ from the b axis, in agreement with the conclusions drawn from the susceptibility results. The fit obtained in Figs. 7 and 8 indicates that within the accuracy of the measurements, each of the two g tensors does have only one nonzero component. However, it is not possible to compare the observed g with the predicted value, as the latter was calculated for the paramagnetic state only and no clearly paramagnetic resonance was observed. Moreover, each of the resonance branches observed in the antiferromagnetic state had a range of g factors from 6.0–12.0. It might be worth noting that the average g value of the ISR branches is 8.0, not very much different from the predicted value of 8.6.

C. ISR

Qualitatively, the weak Fe^{2+} resonances exhibit the behavior expected of the Ising model presented earlier. Four distinct branches have been observed with three associated zero-field splittings. The best fit of the zero-field splittings to the model yields the parameters

$$\begin{aligned} &\Delta/k=0.096\ \text{K},\\ &J_1/k=0,\\ &J_2/k=1.30\ \text{K},\\ &J_3/k=0.64\ \text{K}. \end{aligned} \tag{12}$$

It should be noted that the model predicts four additional branches within the range of the observations to which no observed lines have been assigned, i.e., those corresponding to the zero-field splittings $2J_3$ and $2J_2+2J_3$. There are, however, numerous observed resonance lines which were too weak to be accurately assigned which may account for these branches.

The parameters obtained above may be compared with the values obtained by Uryû. In making this comparison, it is necessary to account for the different magnitudes of the spins. Uryû assigned to the spins a unit length while we have used a pseudospin $S'=\frac{1}{2}$. Thus it is necessary to multiply his values by a factor of 4. This yields the following values:

$$\begin{aligned} &J_1/k=0.020\ \text{K},\\ &J_2/k=0.612\ \text{K},\\ &J_3/k=0.300\ \text{K}. \end{aligned} \tag{13}$$

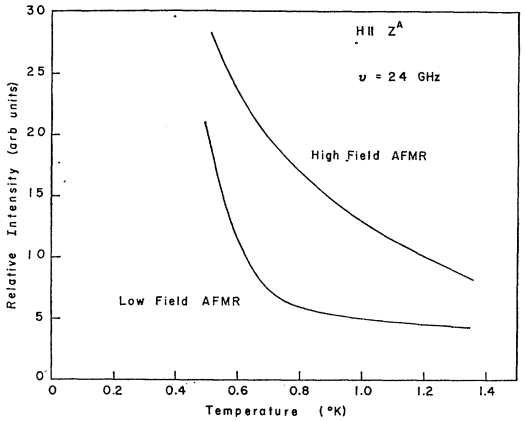

FIG. 13. Temperature dependence of the AFMR absorption intensity. $\nu=24$ GHz.

Although the model seems to produce the main features of the resonance diagram, the ground doublet of the Fe^{2+} cannot explain the wide variation in the observed g values. However, it may be possible to account for these large g shifts by including the effects of the exchange coupling in mixing the excited spin states into the ground doublet. We note that the largest exchange splitting observed was about $2.55k$, while the first excited spin state is $7.92k$ above the ground doublet. Thus, the fraction of the first excited state admixed into the ground state might be as large as 0.3. This is about the same order as the largest observed

$$\frac{|g_{\text{th}}-g_{\text{obs}}|}{g_{\text{th}}}=0.23.$$

A mechanism of this kind has been employed by Silverstein[22] to explain the large g shifts observed in $CoCl_2$, although his discussion does not appear to be directly applicable to the case at hand.

The relatively low signal intensities of the ISR are not surprising in view of the nature of the ground doublet. In the case of exact uniaxial symmetry, the ground states would have been pure $m=\pm 2$ states and the transitions would be completely forbidden. Since the departure from uniaxial symmetry is small in this case, the transition probabilities remain small. The over-all temperature dependence seems to be characteristic of this type of resonance, as it is quite similar to that observed in $FeCl_2$.[3] The nearly exponential decrease of the intensity with temperature shown in Fig. 11 is qualitatively explained by the effect discussed in Sec. IV for the simple antiferromagnetic chain. The sharp decrease with increasing temperature appears to be related to the decrease in long-range order as the transition is approached.

D. AFMR

In Sec. IV, we presented a brief survey of the theory of AFMR. Now we must consider the relation of these

[22] S. D. Silverstein, Phys. Rev. Letters 14, 140 (1965).

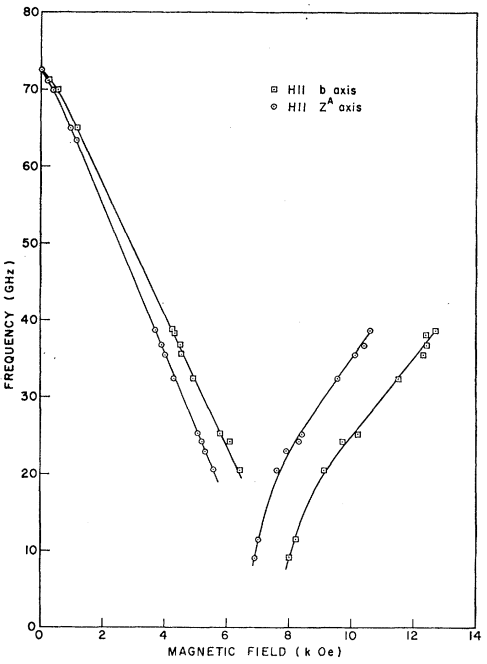

FIG. 14. The frequency-field diagram for the AFMR of the A system plotted for applied field parallel to z^A and to the b axis. The g for the low-field branch is 7.3. Although the high-field branch is curved at low frequencies, it approaches a straight line at high frequencies with a g of 4.3.

theories to the behavior of the intense resonance mode in antiferromagnetic $FeCl_2 \cdot 4H_2O$. The most clearly defined approach is the application of the molecular-field theory to the ground state of the system, proposed by Uryû. However, a comparison of the theoretical and observed frequency-field diagrams indicates that this path leads in the wrong direction. There is, in fact, good reason to believe that the resonance modes observed here are not coupled four-sublattice modes at all, but rather that they arise from two independent, or nearly so, antiferromagnetic systems. Each of these systems corresponds to the inequivalent A and B sublattices, which are then each divided into two antiferromagnetically ordered sublattices.

There are two experimental justifications for this viewpoint. The first rests with the angular dependence: Within the experimental error, the resonances appear to be quite symmetrical about their respective local axes and show no perturbing effect from the other system. The second follows from the presence of two lines arising from each system, which appear to be associated with different magnetic states. The low-field line is clearly the AFMR. It is very intense and relatively narrow ($\sim$200 Oe) below 0.7 K, and diminishes rapidly to a small residual peak on a broad background absorption as the temperature is raised above the Néel point of 1.1 K. In contrast, the high-field line is somewhat broader and more symmetrical, decreases in amplitude more slowly as the temperature is raised and retains its character well above T_N. Consequently, this line is attributed to the high-field-induced paramagnetic state of the individual two-sublattice system with which it is associated. In Fig. 12, the resonance line at 10.5 kOe is the AFMR line associated with the B system, while the other lines are associated with the A system. The important point here is that the B system is still in the antiferromagnetic state, even though the A system is in the high-field paramagnetic state. The broadening of this line arises from the rapid angular dependence at large angles from its local spin axis. This argument shows that the two systems, at least in this regard, behave independently. In view of this conclusion, the rest of the discussion will consider only one of the individual antiferromagnetic systems.

As the foregoing discussion indicates, the identification of the AFMR branches is not completely trivial. The reason for this is that in some respects the AFMR in $FeCl_2 \cdot 4H_2O$ behaves quite unlike that observed in other materials. The most striking departure from "normal" behavior is the lack of temperature dependence of the resonance condition. In general, the molecular-field theory predicts, and experiment supports, that the AFMR frequency will tend to zero as the Néel temperature is approached. This arises from the presence of thermal averages of the spin expectation values in the expressions for the molecular fields. The absence of such behavior here must, in part at least, be attributed to the ease with which the magnetic moments of the Fe ions are saturated. The Mössbauer experiments show that the exchange interaction alone is nearly adequate to saturate the electronic moments at 0.9 K. The presence of applied fields would cause the moments to saturate at even higher temperatures. Furthermore, if the independent two-sublattice model is appropriate, the AFMR would involve only two "nearest neighbors." Consequently, the amount of order required for the existence of AFMR is quite small. This is reflected in the persistence of a small remanent peak at the AFMR frequency above T_N.

Even though the two-sublattice system is more appropriate, attempts to calculate the effective fields, and thus the resonance diagram, meet with the same lack of success that the Uryû model did. The difficulty rests with the large values for the anisotropy field when expression (7) is used along with the value of D given by Schreimpf and Friedberg. It is therefore necessary to resort to a more phenomenological approach in which we use the expression (8) to calculate the uniaxial anisotropy constant K. In the derivation of (8) an isotropic g factor was assumed, but since only the perpendicular components appear in the derivation, it is necessary only to assume that these components are equal, i.e., the g tensor is uniaxial. This condition is nearly, but not exactly satisfied by the g tensor determined from the susceptibility measurements. Consequently, an average value of $g=2.205$ has been used in

the calculation. In addition, it is necessary to halve the value of the perpendicular susceptibility (taken here as χ_c), since there are four, rather than two sublattices. Thus, the value of $\chi_\perp$ to be used is 0.13 (cgs/mole). The resulting value of K is then 3.54×10^7 ergs/mole. Since $\chi_\perp$ and ν are both independent of temperature in the antiferromagnetic state, it follows that K is also temperature-independent.

E. Spin Flop

From the relation for the critical field, we see that the condition for spin flop is $\chi_\perp > \chi_{11}$. In $FeCl_2 \cdot 4H_2O$ this condition is satisfied for temperatures less than 0.65 K. In using (9) to calculate the critical field, the values of χ_{11} and $\chi_\perp$ must be those appropriate to the subsystem, A or B, in question. These may be found by noting that

$$\chi_b = 2\chi_{11}\cos^2 30^\circ + 2\chi_\perp \sin^2 30^\circ ,$$

$$\chi_{a'} = 2\chi_\perp \cos^2 30^\circ + 2\chi_{11}\sin^2 30^\circ ,$$

where χ_b and $\chi_{a'}$ are the macroscopic quantities. The $T=0$ value of H_c obtained in this way is about 23.3 kOe. Since K was shown to the temperature-independent, it would appear that H_c should have the same temperature dependence as $(\chi_\perp - \chi_{11})^{-1/2}$. Since the critical field which separates the two resonance branches is about 6.8 kOe and is roughly temperature-independent, it seems unlikely that the high-field phase of this material is a spin-flop phase in any common sense of the term. Also, as noted in Sec. IV, the derivation of the spin-flop condition assumes an exchange-dominated system. Since it appears from both the resonance and susceptibility results that $FeCl_2 \cdot 4H_2O$ is a system dominated by crystal-field anisotropy, it is not surprising that spin flop is not observed.

Usually, in the spin-flop phase of a uniaxial antiferromagnet there is a resonance mode which had the frequency dependence upon applied field,

$$\nu^2 = (\gamma/2\pi)^2(H_0^2 - H_c^2) , \qquad (14)$$

where γ is the magnetogyric ratio. Of course, as the field is increased above the critical field, the resonance condition approaches that of the paramagnetic ion. In $FeCl_2 \cdot 4H_2O$, however, the resonance condition above the critical field cannot be fitted to the quadratic form above, and the effective g value at high fields approaches a value which is approximately half that associated with the ferrous ground state.

VII. CONCLUSIONS

In the light of the previous discussion in which the resonance results have been compared to various models, it seems clear that there is no single adequate theory which explains all of the resonance phenomena. Nevertheless, an attempt is made here to draw some conclusions regarding the nature of the Fe^{2+} ion and the interactions between the ions, as well as the structure of the magnetic system.

On the basis of specific-heat and magnetic-susceptibility studies conducted in the paramagnetic region, a fairly definite model of the ferrous ion was developed. It was generally expected that magnetic resonance experiments would provide a direct test of this model. Although no paramagnetic resonance was observed, the orientational dependence of the resonances observed in the antiferromagnetic region give credence to the model. In addition, the resonance results verify the orientation of the two local spin axes.

In considering the large deviation from the theoretical g factor of 8.6 associated with the ISR, it was apparent that the simple model of the paramagnetic ion would have to be modified to take into account exchange mixing of the spin states. The ISR seem to be highly localized excitations whose intensity at low temperatures is roughly proportional to the net magnetization. These resonances also present the possibility that there are up to third-nearest-neighbor exchange interactions coupling the four sublattices together as suggested by Uryû.

This conclusion seems to be at odds with the behavior of the intense AFMR. These appear to be associated with two independent two-sublattice systems. It may be, however, that there do exist coupled four-sublattice modes which occur at frequencies above those used in this study. Like the ISR, the AFMR appear to be localized, though perhaps not to the same extent. This is indicated by the temperature independence of the resonance condition as well as the persistence of a residual absorption at the AFMR frequency above the critical temperature.

The nature of the high-field state of the magnetic system remains relatively undefined. The results presented here would indicate that the high-field state is paramagnetic in that there was no sharp or discontinuous change in the behavior of the high-field resonance branch as the temperature was varied from 0.4 to 1.5 K. Recent adiabatic magnetization results, however, indicate that there is a spin-flop state below 0.75 K in fields above 5.5 kOe. Thus, it appears that $FeCl_2 \cdot 4H_2O$ merits further study.

ACKNOWLEDGMENTS

I would like to express my debt to Professor A. Honig for the stimulus and guidance which he provided throughout the course of this work. I would like to thank Professor G. Wessel for the loan of his 35- and 70-GHz klystrons. I am also grateful to Dr. B. W. Mangum and NBS for permitting the pure-sample and X-band ISR results to be published here.